Table IV. Enthalpies of Vitrification of Crystalline Framework Aluminosilicates

M	x	Structure	ΔH_{vit} (kJ per 2 mol oxygen)
	0	β-quartz	7.0*
Rb	0.250	Microcline	10.2†
K	0.250	High sanidine	12.0*
Na	0.250	High albite	13.0*
	0.500	Nepheline	12.8*
Li	0.500	Eucryptite	16.9†
Ca	0.500	Anorthite	19.5*
Mg	0.445	Cordierite	25.1*

*Reference 12. †Present work, as discussed in text.

coordination number 6 for Li and Mg and 8 for the other ions. Though the choice of charge and size is rather arbitrary, the ionic potential offers a reasonable parameter, easily calculated for all ions, for comparing the relative bonding strength of different cations. The correlation in Fig. 4, though curved rather than linear, shows clearly that the stability of aluminosilicate glasses is inversely related to the ability of M to bond to oxygen.

The enthalpy difference between crystal and glass (enthalpy of vitrification), ΔH_{vit}, is listed in Table IV for SiO_2 and a number of framework silicates. Figure 4 also shows a linear correlation of ΔH_{vit} with z/r. If one considers silica (quartz and glass) as a framework structure with the interstices occupied by a cation (i.e., a vacancy) of infinitely weak ability to perturb the bridging oxygen, then the point for SiO_2 with $z/r = 0$ lies on the same trend as the framework aluminosilicates. The heat of vitrification increases with increasing z/r, indicating that increasing perturbation of the aluminosilicate framework decreases the stability of the glass not only with respect to mixing properties in the amorphous state but also with respect to the crystalline state.

Acknowledgments: We thank J. Clark, R. Hervig, and A. Yates for help with chemical analyses and L. Briley and C. Skiba for maintenance of equipment.

References

[1]H. J. Byker, R. E. R. Craig, I. Eliezer, N. Eliezer, R. A. Howald, and P. Viswanadham, "Thermodynamic Treatments of the CaO-SiO_2 System," *CALPHAD: Computer Coupling Phase Diagrams Thermochem.*, **5** [3] 217–224 (1981).
[2]N. Eliezer, R. A. Howald, M. Marinkovic, and I. Eliezer, "Vapor Pressure Measurements, Thermodynamic Parameters, and Phase Diagram in the System Potassium Oxide-Silicon Oxide at High Temperatures," *J. Phys. Chem.*, **82** [9] 1021–1028 (1978).
[3]I. Eliezer, N. Eliezer, R. A. Howald, M. C. Verwolf, and P. Viswanadham, "The Enthalpy of Sodium Silicate Glasses and Liquids," *CALPHAD: Computer Coupling Phase Diagrams Thermochem.*, **3** [1] 1–8 (1979).
[4]T. Ostvold and O. J. Kleppa, "Thermochemistry of the Liquid System Lead Oxide-Silica at 900°C," *Inorg. Chem.*, **8** [1] 78–82 (1969).
[5]R. H. Rein and J. Chipman, "Activities in the Liquid Solution SiO_2-CaO-MgO at 1600°C," *Trans. Metall. Soc. AIME*, **233** [2] 415–425 (1965).
[6]D. R. Gaskell, "The Thermodynamic Properties of the Masson Polymerization Model of Liquid Silicates," *Metall. Trans.*, **4** [1] 185–193 (1973).
[7]R. J. Charles, "Origin of Immiscibility in Silicate Solutions," *Phys. Chem. Glasses*, **10** [5] 169–178 (1969).
[8]M. Taylor and G. E. Brown, Jr., "Structure of Mineral Glasses I. The Feldspar Glasses $NaAlSi_3O_8$, $KAlSi_3O_8$, $CaAl_2Si_2O_8$," *Geochim. Cosmochim. Acta*, **43** [1] 61–74 (1979).
[9]M. Taylor and G. E. Brown, Jr., "Structure of Mineral Glasses II. The SiO_2-$NaAlSiO_4$ Join," *Geochim. Cosmochim. Acta*, **43** [9] 1467–1473 (1979).
[10]F. A. Seifert, B. O. Mysen, and D. Virgo, "Three-Dimensional Network Structure of Quenched Melts (Glass) in the Systems SiO_2-$NaAlO_2$, SiO_2-$CaAl_2O_4$ and SiO_2-$MgAl_2O_4$," *Am. Mineral.*, **67** [7–8] 696–717 (1982).
[11]P. F. McMillan, B. Piriou, and A. Navrotsky, "A Raman Spectroscopic Study of Glasses Along the Joins Silica-Calcium Aluminate, Silica-Sodium Aluminate, and Silica-Potassium Aluminate," *Geochim. Cosmochim. Acta*, **46** [11] 2021–2037 (1982).
[12]A. Navrotsky, G. Peraudeau, P. McMillan, and J. P. Coutures, "A Thermochemical Study of Glasses and Crystals Along the Joins Silica-Calcium Aluminate and Silica-Sodium Aluminate," *Geochim. Cosmochim. Acta*, **46** [11] 2039–2047 (1982).
[13]A. Navrotsky, R. Hon, D. F. Weill, and D. J. Henry, "Thermochemistry of Glasses and Liquids in the Systems $CaMgSi_2O_6$-$CaAl_2Si_2O_8$-$NaAlSi_3O_8$, SiO_2-$CaAl_2Si_2O_8$-$NaAlSi_3O_8$ and SiO_2-Al_2O_3-Na_2O," *Geochim. Cosmochim. Acta*, **44** [10] 1409–1423 (1980).
[14]R. L. Hervig and A. Navrotsky, "Thermochemical Study of Glasses in the System $NaAlSi_3O_8$-$KAlSi_3O_8$-Si_4O_8 and the Join $Na_{1.6}Al_{1.6}Si_{2.4}O_8$-$K_{1.6}Al_{1.6}Si_{2.4}O_8$," *Geochim. Cosmochim. Acta*, **48** [3] 513–522.
[15]G. Peraudeau and A. Navrotsky, "Calorimetry of Glasses in the System $Mg_{0.5}AlO_2$-SiO_2"; unpublished work.
[16]A. Navrotsky, "Recent Progress and New Directions in High Temperature Calorimetry," *Phys. Chem. Miner.*, **2** [1–2] 89–104 (1977).
[17]A. Navrotsky, K. L. Geisinger, P. McMillan, and G. V. Gibbs, "Implications of Molecular Orbital Calculations on Tetrahedrally Bonded Clusters for the Structure, Thermodynamics, and Physical Properties of Glasses and Melts in Silicate, Aluminosilicate, Borosilicate, and Other Related Systems"; unpublished work.
[18]R. D. Shannon and C. T. Prewitt, "Effective Ionic Radii in Oxides and Fluorides," *Acta Crystallogr., Ser. B*, **B25** [5] 925–946 (1969).

Thermodynamic Investigations in the System U-Mo-O

G. CHATTOPADHYAY, S. N. TRIPATHI, and A. S. KERKAR

Water Chemistry Division, Bhabha Atomic Research Centre, Bombay 4 00 085, India

The phase diagram of the system U-Mo-O in the region UO_2-MoO_2-O was investigated by X-ray phase analysis and electromotive force measurements. The isothermal section at 1000 K is presented. The free energy of formation of $UMoO_5$ was determined from the oxygen potential measurement by a $ZrO_2 \cdot CaO$ solid electrolyte galvanic cell. This gave at 1000 K

$$^f\Delta G^\circ\langle UMoO_5\rangle = -1424.7 \pm 1 \text{ kJ} \cdot \text{mol}^{-1}$$

A redetermination of the free energy of formation of MoO_2 yielded (ΔG in kJ · mol^{-1})

$$^f\Delta G^\circ\langle MoO_2\rangle = -566.174 + 0.1615T \pm 0.4$$

for 1040 to 1290 K. The free energies of formation of three other phases were calculated using the key values from the literature, $^f\Delta G^\circ\langle UMoO_5\rangle$, $^f\Delta G^\circ\langle MoO_2\rangle$, and the phase diagram obtained in the present investigation. The values at 1000 K are

$$^f\Delta G^\circ\langle UMoO_6\rangle = -1476 \pm 12 \text{ kJ} \cdot \text{mol}^{-1}$$

$$^f\Delta G^\circ\langle U_2MoO_8\rangle = -2433 \pm 8 \text{ kJ} \cdot \text{mol}^{-1}$$

$$^f\Delta G^\circ\langle UMo_2O_8\rangle = -1918 \pm 10 \text{ kJ} \cdot \text{mol}^{-1}$$

From the present investigation it was concluded that ternary phases of the system U-Mo-O will not play any role in the fission product-fuel interaction, while in the nuclear waste calcine, only $UMoO_6$ could be of importance. A vaporization study of the latter phase has been suggested.

I. Introduction

THERMODYNAMIC data on materials are required to answer some practical questions regarding chemical equilibria and also for the ultimate purpose of quantifying the relative stabilities of all possible chemical species.

The present work was undertaken to determine what role molybdenum, one of the most preponderant fission products, could play in determining the state of the chemical equilibrium in the fuel fission product complex in an oxide-based nuclear reactor or in the nuclear waste disposed in ceramic or glass forms. To understand and analyze such complex systems, it is necessary to know which are the possible phases and species that are to be considered and their thermodynamic properties.

In the present work attention was given to the ternary oxides of uranium and molybdenum with regard to the equilibria among the various phases. This is a prerequisite for determining the thermodynamic properties of the relevant phases. Therefore, experiments were carried out to construct the phase diagram in the region UO_2-MoO_2-O in a more precise manner than hitherto and, hence, to determine the free energy of formation of $UMoO_5$.

Received December 14, 1983; revised copy received April 9, 1984; approved May 10, 1984.

II. The System U-Mo-O

The U-Mo binary phase diagram containing only one intermetallic phase is known.[1] The Mo-UO_2 cermets were thoroughly investigated because of the attention they drew as a potential nuclear fuel.[2] Keller[3] dealt with the ternary phases in an up-to-date review of the system U-Mo-O. The ternary crystalline phases, along with their crystallographic data, are listed in Ref. 4. The ternary phase diagram in the region UO_2-MoO_2-MoO_3[5] at T = 700° to 750°C shows six ternary phases, namely $UMoO_6$, U_2MoO_8, $UMoO_5$, UMo_2O_8, UMo_7O_{22}, and $UMo_{11}O_{35}$. In addition, $U_3Mo_{20}O_{64}$ in three modifications (α, β, γ) and $UMo_{10}O_{32}$[6,7] have been reported. Most probably, β-$U_3Mo_{20}O_{64}$ is identical with UMo_7O_{22} and $UMo_{10}O_{32}$ with $UMo_{11}O_{35}$.[3] The latter could also be a solid solution of $UMo_{10}O_{32}$ and MoO_3. The phase $UMoO_6$ forms a eutectic with MoO_3 at 742°C and decomposes peritectically at 980°C.[8] $UMoO_5$ decomposes peritectically at 1087°C. UMo_2O_8 undergoes a phase transition at 1000°C and melts peritectically at 1040°C, whereas $UMo_{11}O_{35}$ decomposes peritectically at 830°C.[9] The temperatures up to which the α- and γ-$U_3Mo_{20}O_{64}$ remain crystalline are not known.

III. Experimental Procedure

(1) Materials

Starting materials for phase investigations were MoO_3,* nuclear-grade U_3O_8, and molybdenum powder (purity >99.9%). The last two were obtained from the Atomic Fuels Division and the Metallurgy Division of this centre, respectively.

Iron and nickel sponges, Fe_2O_3 and NiO, were the starting materials† for preparing reference electrodes in the galvanic cell studies.

(2) Phase Analysis

A compacted mixture of U_3O_8 and MoO_3 in a 1:1 molar ratio heated in air at 873 K for 6 h yielded pure $UMoO_6$. $UMoO_5$ was prepared by heating a compacted equimolar mixture of UO_2 and MoO_3 in a sealed evacuated quartz ampoule at 1200 K for 200 h. UO_2 was prepared beforehand by hydrogen reduction of U_3O_8. Subsequently U_3O_8, MoO_3, Mo, $UMoO_6$, and $UMoO_5$ were mixed in various proportions and compacted into pellets. The compacted pellets were heat-treated in sealed, evacuated silica ampoules at 1200 K for 200 h. The phases in the heat-treated samples were identified by X-ray diffractometry of the powders. The phases richer in MoO_3 could not be prepared this way because of the massive losses of MoO_3, as seen in the attack of the silica ampoules. All samples were further heated at 1000 K in a flow of purified argon for 60 h and the phases were again identified.

(3) Galvanic Cell Measurement

The emf of a series of solid electrolyte galvanic cells with calcia-stabilized zirconia‡ were measured in order to determine the stoichiometry of the uranium oxide coexisting in the three-phase regions of the phase diagram. The experimental setup and the gas purification system were similar to the ones described earlier.[10,11] The emf of the following cells was measured.

*Analytical-reagent grade, J. T. Baker Chemical Co., Phillipsburg, NJ.
†Specpure, Johnson, Mathey & Co., Inc., New York, NY.
‡Friederichsfeld, Mannheim, Federal Republic of Germany.

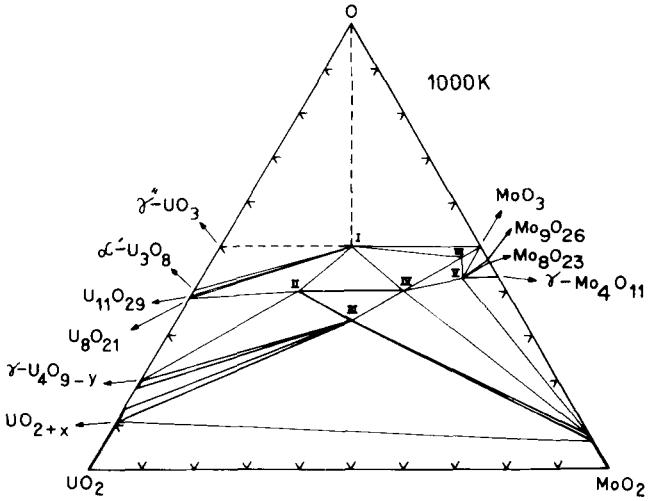

Fig. 1. Isothermal section of phase diagram of system UO_2-MoO_2-O at 1000 K. I = $UMoO_6$, II = U_2MoO_8, III = $UMoO_5$, IV = UMo_2O_8, V = UMo_7O_{22}, and VI = $UMo_{11}O_{35}$.

(I) Pt/Mo/Fe, FeO/ZrO_2·CaO/Fe, FeO/Mo/Pt

(II) Pt/Mo, MoO_2/ZrO_2·CaO/Fe, FeO/Mo/Pt

(III) Pt/Mo, MoO_2, UO_2/ZrO_2·CaO/Fe, FeO/Mo/Pt

(IV) Pt/Fe, FeO/ZrO_2·CaO/UO_{2+x}, MoO_2, $UMoO_5$/Pt

(V) Pt/Ni, NiO/ZrO_2·CaO/UO_{2+x}, MoO_2, $UMoO_5$/Pt

The reference electrodes Fe, FeO and Ni, NiO and the test electrode Mo, MoO_2 were prepared by mixing metal powders with their corresponding oxides Fe_2O_3, NiO, and MoO_3, respectively, in appropriate proportions so as to give the final metal-to-oxide in a 1:1 molar ratio. They were compacted into 6-mm-diameter pellets and sintered in vacuum at 1273 K for 4 h.

The test electrode of cell (III) was prepared by pelletizing a mixture of Mo and partially reduced U_3O_8 in a 2:1 molar ratio and sintering in vacuum at 1200 K for 200 h. The coexistent phases were identified in the electrode pellets by X-ray diffractometry. The test electrode in cells (IV) and (V) was the product obtained in the earlier phase analysis experiments.

Cells (I) to (III) were assembled by direct stacking of the pellets. Cells (IV) and (V) were assembled by enclosing the right-hand electrode in powder form in a calcia-stabilized zirconia crucible by a glass seal, as was adopted in an earlier work.[11] This was needed because the mixture of UO_2, MoO_2, and $UMoO_5$ was not compactable. Moreover, the gas-phase interactions and volatilization could thus be avoided.

IV. Results

(1) Phase Diagram

The starting materials, their molar ratios, and the phases identified after equilibration are given in Table I. The isothermal section at 1000 K of the UO_2-MoO_2-O region of the U-Mo-O ternary is presented in Fig. 1. In Table I, the phase U_8O_{21} has been written

Table I. Identification of Coexisting Phases in the System U-Mo-O

Starting material	Product	
	1200 K (vacuum)	1000 K (argon)
U_3O_8 + MoO_3 (1:1)	U_3O_8, $UMoO_6$, U_2MoO_8	U_3O_8, $UMoO_6$, U_2MoO_8
U_3O_8 + $UMoO_5$ (3:8)	U_3O_8, U_4O_9, U_2MoO_8	U_3O_8, U_4O_9, U_2MoO_8
$UMoO_6$ + Mo (1:1)	$UMoO_5$, MoO_2, UO_{2+x}	$UMoO_5$, MoO_2, UO_{2+x}
U_3O_8, MoO_3, Mo (6:29:7)	U_3O_8 + U_2MoO_8	
$UMoO_6$ + UO_2 (1:2.5)	U_4O_9 + U_2MoO_8	
$UMoO_5$		$UMoO_5$ + U_2MoO_8
$UMoO_6$ + MoO_3 (1:1)		$UMoO_6$ + MoO_3 + $UMo_{11}O_{35}$*
UO_2 + MoO_3 (2:1)		UO_2 + $UMoO_5$ (vacuum)

*Three types of crystals could be seen under the microscope.

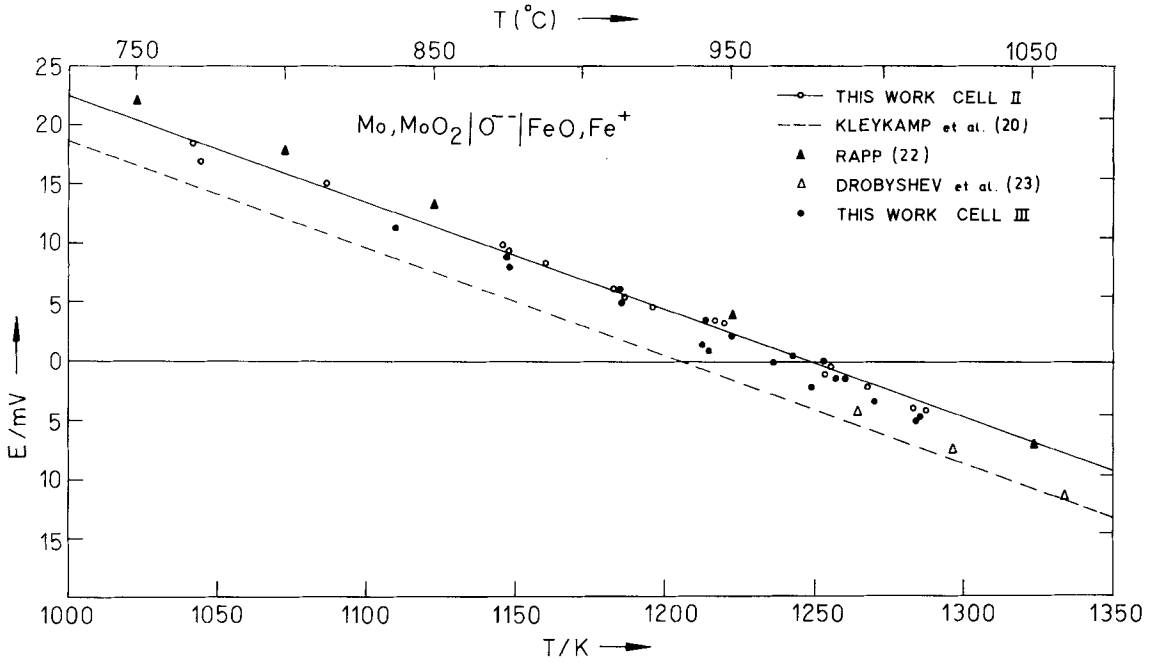

Fig. 2. Electromotive force for cells I, II, and III as a function of temperature.

Table II. Emf of Cell (IV) at Various Temperatures

Run 1				Run 2	
T (K)	E (mV)	T (K)	E (mV)	T (K)	E (mV)
1001	471.3	929	485.8	1003	472.7
982	474.9	953	477.7	988	476.3
986	473.3	969	476.3	1000	474.9
971	478.1	986	474.4		
954	483.6	1002	471.3		
		1017	472.7		

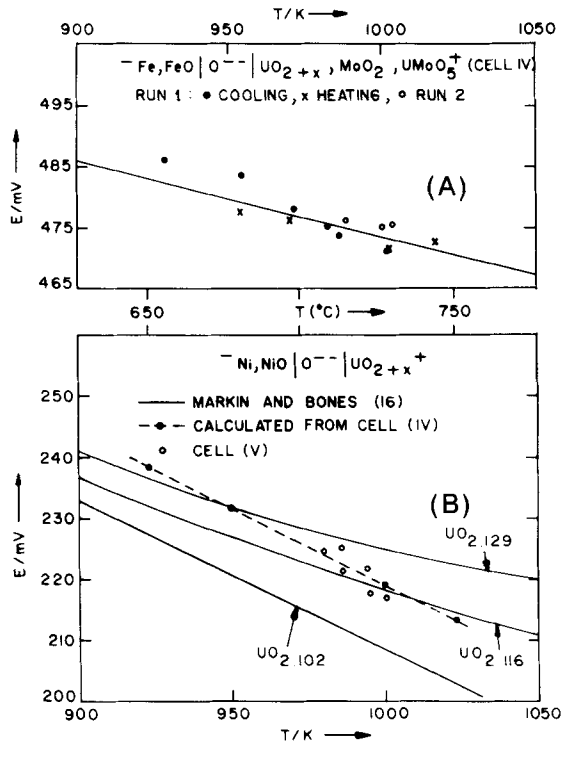

Fig. 3. Electromotive force for cells (*A*) IV and (*B*) V (with data from Ref. 16) as a function of temperature.

as U_3O_8 because in the multiphase X-ray diffraction pattern the other homologous phases could not be distinguished from α-U_3O_8.

The homogeneity ranges of the binary phases in the systems U-O and Mo-O were taken from Refs. 12 and 13. The region on the right-hand side of the phase UMo_2O_8 in Fig. 1 is taken from Refs. 5 and 14. The two-phase regions are drawn assuming that the phases $UMoO_6$, U_2MoO_8, and $UMoO_5$ do not have any appreciable range of homogeneity. The X-ray diffraction peaks of these phases in various two- and three-phase mixtures did not show any shift corroborating this assumption.

The composition of the UO_{2+x} phase, which is at equilibrium with MoO_2 and $UMoO_5$, was determined from the emf of cells (IV) and (V) (see Section IV(2)).

(2) Emf Measurement

The emf of cell (I) was measured between 1000 and 1300 K. This gave an emf of ±0.5 mV over the entire temperature range.

The emf of cell (II) as a function of temperature is given by Eq. (1) (E in mV)

$$E_{II} = (112.9 \pm 2.1) - (0.09048 \pm 0.00180)T \quad (1)$$

for 1040 to 1290 K and is plotted in Fig. 2 along with the emf of cell (III) as well as the literature data.

The emf of cell (IV) at various temperatures is given in Table II and is presented in Fig. 3(*A*).

The emf of cell (V) is superimposed in Fig. 3(*B*) on the emf vs temperature plots for three selected compositions $UO_{2.129}$, $UO_{2.116}$, and $UO_{2.102}$ of nonstoichiometric uranium dioxide taken from the work of Markin and Bones.[16]

The free energy of formation of MoO_2 was calculated from Eq. (1) using the free energy of formation of Fe_xO[15] and is given by Eq. (2) (ΔG in kJ·mol^{-1}):

$$^{f}\Delta G^{\circ}\langle MoO_2\rangle = -566.174 + 0.1615T \pm 0.4 \quad (2)$$

for 1040 to 1290 K.

The composition of uranium dioxide coexisting with MoO_2 and $UMoO_5$ at 1000 K can be read out from Fig. 4, which was constructed from Ref. 16 and which serves as the calibration curve for the composition in UO_{2+x} in terms of the emf of the cell: Ni, $NiO/ZrO_2 \cdot CaO/UO_{2+x}$. At 1000 K, the composition of the nonstoichiometric oxide in equilibrium with MoO_2 and $UMoO_5$ is found to be $UO_{2.115}$ (see Fig. 4). In contrast, the lattice pa-

rameter measurements yielded a value of $a = 544$ pm, which corresponded to the composition $UO_{2.25}$. In Fig. 3(*B*) the results of cell (IV) are also shown by combining the emf of cell (IV) with the free energy of formation of nickel oxide[17] (dashed line). At 1000 K the emf of cell (V) and that calculated from cell (IV) are identical. At lower temperatures, it appears that the composition of UO_{2+x} shifts toward the oxygen-rich side. This explains the difference in the results of the X-ray and emf measurements. It should be noted that, at $T < 1000$ K, very large equilibration time and considerable hysteresis were observed, indicating a change in composition of uranium dioxide with changing temperature.

The free energy of formation of $UMoO_5$ is calculated from the equilibrium

$$UO_{2.115} + MoO_2 + 0.4425O_2 = UMoO_5 \quad (3)$$

This gives

$${}^f\Delta G^\circ\langle UMoO_5\rangle = {}^f\Delta G^\circ\langle UO_{2.115}\rangle + {}^f\Delta G^\circ\langle MoO_2\rangle + 0.4425\overline{\Delta G}_{O_2} \quad (4)$$

The value of $\overline{\Delta G}_{O_2}$ was determined from the emf of cells (IV) and (V). The value of ${}^f\Delta G^\circ\langle UO_{2.115}\rangle$ was evaluated by the Gibbs-Duhem integration in the form:

$${}^f\Delta G^\circ\langle UO_{2+x}\rangle = {}^f\Delta G^\circ\langle UO_2\rangle + \frac{1}{2}\left(x\overline{\Delta G}_{O_2}^{NiO/Ni} + 4F\int_0^x E dx\right) \quad (5)$$

where $\overline{\Delta G}_{O_2}^{NiO/Ni}$ is the relative partial molar free energy of oxygen of the reference electrode of the cell, Ni, $NiO/O^{2-}/UO_{2+x}$, E the corresponding emf, and F the Faraday constant. The integration could be directly performed on the curve shown in Fig. 4, which gives E as a function of x[16]; ${}^f\Delta G^\circ\langle UO_2\rangle$ was taken from Ref. 18. The free energy of formation of MoO_2 was evaluated by extrapolating our data given by Eq. (2) to 1000 K. This yielded ${}^f\Delta G^\circ\langle UMoO_5\rangle = -1424.7 \pm 1$ kJ·mol^{-1}.

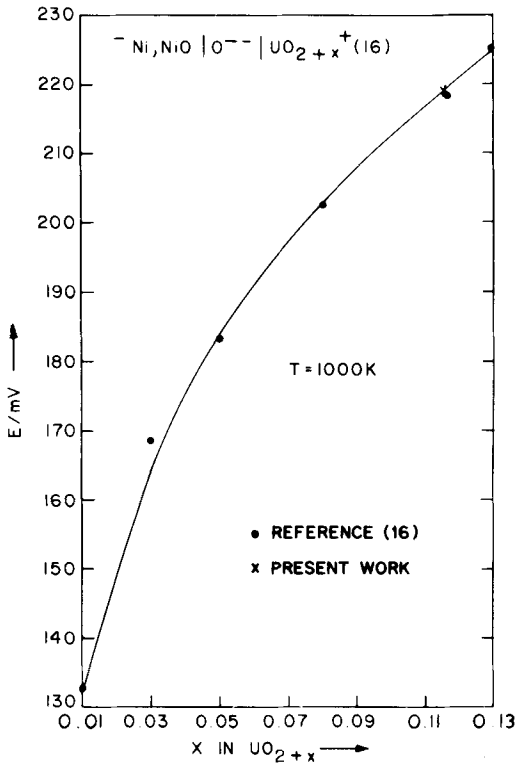

Fig. 4. Emf vs composition isotherm at 1000 K for nonstoichiometric uranium dioxide with Ni, NiO as reference electrode (Ref. 16).

V. Discussion

Determination of the free energy of formation of $UMoO_5$ necessitated knowledge of the free energy of formation of MoO_2 according to Eq. (4). The free energy of formation data of MoO_2 from various investigations are listed in Refs. 19–21. There are some disagreements. To ascertain the extent of the disagreement we compared our results in Fig. 2 with those emf data from the literature in which Fe, Fe_xO was used as the reference electrode.[20,22,23] Comparison with the recent results of Ref. 24 was not possible because the authors did not give the emf values. As will be seen from Fig. 2, our values lie close to that of Ref. 22 while the values of Ref. 23 are closer to those of Ref. 20. In the present study we noticed that, at lower temperatures, the emf tended to drift toward lower values. This drift was more pronounced when the Mo, MoO_2 pellet was used without prior polishing (on 600 μm carborundum paper). For further confirmation of our results of cell (II), we measured the emf of cell (III), which is also plotted in Fig. 2. The emf of cell (III) with the unpolished surface was about 1 mV less than that of cell (II). But on prior polishing the emf of cell (III) became identical with that of cell (II) down to 1150 K, below which cell (III), even with the polished pellet, showed some difference. The emfs shown in Fig. 2 were recorded when the drift in emf was <0.5 mV in 12 h. Since the emf of cells (II) and (III) is close to zero mV, we measured the symmetric cell (I) as an additional test of reliability of our data. In our measurements we used molybdenum disks as the contact lead because, from the thermodynamic point of view, Mo should be more inert toward Fe, Fe_xO than Pt.[25,26] In the initial stages of our measurement, the emf showed a small dependence on the gas flow rate which could be rectified by placing a pure iron wire upstream and Fe, Fe_xO pellets in a combustion boat near the cell location.

Comparison of the emf of cells (II) and (III) confirms that there is no mutual solid solubility between UO_2 and MoO_2.

The emf of cell (IV), presented in Table II, shows immediately that the data are consistent with the phase diagram (Fig. 1) in that the emf of cell (IV) is less negative than that of the cell Fe, $FeO/ZrO_2 \cdot CaO/MoO_2 \cdot Mo_4O_{11}$ measured by Ref. 20. The reliability of the results of cell (IV) is further ensured from the consistency with those of cell (V), as seen in Fig. 3(*B*).

The phase diagram presented in Fig. 1 was obtained by combining our phase analysis results of Table I with those of Refs. 5 and 14 and with the results of our emf measurements. Our phase diagram differs from that of Ref. 14 in that U_4O_9 coexists with U_2MoO_8 and $UMoO_5$ rather than with U_2MoO_8 and UMo_2O_8 as observed in Ref. 14. Additional evidence in support of this comes from the fact that, when we heated a mixture of $UO_2 + MoO_3$ (1:1) in order to prepare $UMoO_5$ below 1000 K (200 h), we obtained a mixture of U_3O_8, U_4O_9, $UMoO_5$, and U_2MoO_8. When this sample was heated for a further 200 h at 800°C, the product contained $UMoO_5$ and small amounts of U_2MoO_8 and U_4O_9.

From the present value of the ${}^f\Delta G^\circ$ of $UMoO_5$, coupled with the constraints of the present phase diagram, it was possible to estimate the free energies of formation of the three other most important phases, namely, $UMoO_6$, U_2MoO_8, and UMo_2O_8. In Table III we give the upper and lower limits of ${}^f\Delta G^\circ$ required to satisfy the various constraints of the phase diagram.

In drawing the phase diagram (Fig. 1) it was difficult by any conceivable experimental method to establish unequivocally if the two-phase mixture $UO_{2.15} + \gamma\text{-}U_4O_9$, where $UO_{2.15}$ is the equilibrium phase-boundary composition of UO_{2+x} phase,[16,27] should coexist with $UMoO_5$ or U_2MoO_8. Using the free energy data of the present work, we considered the two competing equilibria

$$UMoO_5 + 0.075O_2 = UO_{2.15} + MoO_3(g) \quad (6)$$

$$U_2MoO_8 = 2UO_{2.15} + 0.35O_2 + MoO_3(g) \quad (7)$$

The oxygen potential being the same in both the cases, the stable equilibrium will be that which corresponded to the lower partial pressure of $MoO_3(g)$. The present calculation showed that the phase mixture $UMoO_5 + UO_{2.15} + U_4O_9$ is marginally more stable (by 2 kJ) than $U_2MoO_8 + UO_{2.15} + U_4O_9$.

Table III. Thermodynamic Stability Limits of Phases $UMoO_6$, U_2MoO_8, and UMo_2O_8 at 1000 K

Phase	${}^fΔG°$ (kJ·mol^{-1})	Reaction	Constraint (kJ·mol^{-1})
$UMoO_6$	>-1488	$\frac{1}{3}U_3O_8 + MoO_3 + \frac{1}{6}O_2 = UMoO_6$	$-164.8 < \Delta\bar{G}_{O_2} < -13.4$
	<-1465		
U_2MoO_8	>-2442	$UMoO_5 + \frac{1}{4}U_4O_9 + \frac{3}{8}O_2 = U_2MoO_8$	$-199.3 < \Delta\bar{G}_{O_2} < -164.8$
	<-2425		
UMo_2O_8	>-1938	$UMo_2O_8 + UO_2 = 2UMoO_5$	$-1938 < {}^fΔG°\langle UMo_2O_8\rangle$
	<-1918	$UMoO_5 + MoO_2 + \frac{1}{2}O_2 = UMo_2O_8$	$-177 > \Delta\bar{G}_{O_2}$

Key values of ${}^fΔG°$ at 1000 K from Ref. 18 are -2911 ± 12 for U_3O_8, -3754 ± 12 for U_4O_9, -912 ± 12 for UO_2, and -490 ± 12 for MoO_3.

A similar calculation for the oxygen potential for the two competing equilibria

$$3UMoO_5 + 0.5O_2 = U_2MoO_8 + UMo_2O_8 \quad (8)$$

$$2UMoO_5 + 0.125O_2 = UMo_2O_8 + 0.25U_4O_9 \quad (9)$$

for which partial pressures of $MoO_3(g)$ would be the same shows that the stable equilibrium is represented by Eq. (8). Hence, the phase diagram is consistent with the present set of data. The uncertainties quoted in the present paper for the free energies of formation are based on the estimated error of the measurements and calculations in this work alone and do not include the uncertainties in the key data.

The foregoing results are relevant to the prediction of the chemical state of molybdenum, which has a diagnostic value in the determination of the radial oxygen profile of irradiated fuel material[28,29] in a typical mixed-oxide fuel pin of the FBR type at high burnup. In the present case, the question was whether it is possible that any of the ternary U-Mo-O phases could form inside a fuel pin in which, typically, a temperature gradient of 1000 to 2500 K prevails. The phase diagram in Fig. 1 shows that at 1000 K the lowest oxygen potential at which any of the ternary phases could exist is that corresponding to $UO_{2.115}$ and the phase is $UMoO_5$. The oxygen potential inside a fuel pin is much lower, considering that the starting O/M ratio of the fuel is near stoichiometric or slightly hypostoichiometric. Hence, none of the ternary U-Mo-O phases can form, at least up to 1000 K. This reasoning can be extended to higher temperatures on the basis of Fig. 3(*B*). It can be roughly assumed that even at higher temperatures the O/M ratio of UO_{2+x} coexisting with $UMoO_5$ and MoO_2 will not be less than 2.10, which once again is much larger than that prevailing in the fuel pin, even after taking care of the mass balance and oxygen redistribution after fission.

The present phase diagram also shows that, in the immobilization of high-level liquid wastes in ceramic form by drying, and calcining typically at 750°C in air,[30] the only ternary phase that can appear is $UMoO_6$. The stability of this phase at higher temperatures will have to be established, however, by a separate vaporization study, the results of which are to be presented soon.

VI. Conclusions

(1) Measurement of the emf of cells (II) and (III) confirms that UO_2 and MoO_2 have negligible mutual solid solubility.

(2) From the isothermal section at 1000 K of the system UO_2-MoO_2-O and from the free energy of formation of $UMoO_5$ it can be concluded that $UMoO_5$ cannot form as a reaction product between the fuel (UO_2) and the fission product (Mo) in a reactor, nor should $UMoO_5$ be expected as a component phase in the ceramic waste form.[30]

(3) The only ternary phase in the system U-Mo-O that can form as a component phase in the ceramic waste form is $UMoO_6$. A vaporization study on this phase will shortly be published.

Acknowledgments: The authors thank C. K. Gupta of the Metallurgy Division for the Mo powder, the Atomic Fuels Division for the uranium oxide, and R. G. Yeotikar of the Waste Management Division of this Centre for the aluminum-rich glass powder.

References

[1]P. Chiotti, V. V. Akhachinskij, I. Ansara, and M. H. Rand; p. 144 in The Chemical Thermodynamics of Actinide Elements and Compounds, Part 5. The Actinide Binary Alloys. International Atomic Energy Agency, Vienna, 1981.
[2]E. Gebhardt and G. Ondracek, "Structure of the Uranium Oxide-Molybdenum System," *J. Nucl. Mater.*, **13** [2] 220–28 (1964).
[3]C. Keller; pp. 324–27 in Gmelin Handbuch des Anorganischen Chemie 8. Auflage, Uran Teil C 3. Springer-Verlag, New York, 1975.
[4]K. Girgis; pp. 550–51, Part III-2 in "Molybdenum: Physico Chemical Properties of its Compounds and Alloys," *Atomic Energy Rev., Special Issue*, No. 7. Edited by L. Brewer. International Atomic Energy Agency, Vienna, 1980.
[5]L. M. Kovba and V. K. Turnov, "X-ray Diffraction Studies of Double Oxides in the System UO_2-MoO_2-MoO_3," *Radiokhimiya*, **7**, 316–19 (1965).
[6]V. N. Serezhkin, L. M. Kovba, and V. K. Turnov, "Structure of Uranium and Molybdenum Double Oxides," *Dokl. Akad. Nauk, SSSR*, **210** [5] 1106–1109 (1973).
[7]V. N. Serezhkin, G. N. Ronami, L. M. Kovba, and V. K. Turnov, "New Double Oxides of Uranium and Molybdenum," *Russ. J. Inorg. Chem.*, **19** [4] 565–67 (1974).
[8]O. A. Ustinov, M. A. Andrianov, N. T. Chebotarev, and G. P. Novoselov, "Molybdenum Trioxide-Uranium Trioxide System," *Sov. At. Energy (Eng. Transl.)*, **34**, 155–57 (1973).
[9]O. A. Efremova, V. K. Turnov, and L. M. Kovba, "Thermal Study of the System UO_2-MoO_3," *Radiokhimiya*, **9**, 141–43 (1967).
[10]H. Kleykamp, "Free Enthalpy of Formation of Palladium Oxide," *Z. Phys. Chem.*, **71** [1–3] 142–48 (1970).
[11]G. Chattopadhyay and H. Kleykamp, "Phase Equilibria and Thermodynamic Studies in the Titanium-Nickel and Titanium-Nickel-Oxygen System," *Z. Metallkde*, **74** [3] 182–87 (1983).
[12]D. K. Smith, B. E. Scheetz, C. E. F. Anderson, and K. L. Smith, "Phase Relations in the Uranium-Oxygen-Water System and its Significance on the Stability of Nuclear Waste Forms," *Uranium*, **1**, 79–111 (1982).
[13]L. Brewer and R. H. Lamoreaux; p. 285, Part II in *Atomic Energy Rev., Special Issue*, No. 7. Edited by L. Brewer. International Atomic Energy Agency, Vienna, 1980.
[14]V. K. Turnov, O. N. Rozanova, and L. M. Kovba, "A Double Oxide of Uranium and Molybdenum," *Russ. J. Inorg. Chem.*, **10** [11] 1400–1401 (1965).
[15]H. F. Rizzo, R. S. Gordon, and I. B. Cutler, "Determination of Phase Boundaries and Thermodynamic Functions in the Iron-Oxygen System by EMF Measurements," *J. Electrochem. Soc.*, **116** [2] 266–74 (1969).
[16]T. L. Markin and R. J. Bones, "The Determination of Changes in Free Energy for Uranium Oxides Using a High Temperature Galvanic Cell," Part I. AERE–R 4042 (1962).
[17]S. Berglund, "The Free Energy of Formation of Nickel Oxide," *Ber. Bunsengesells.*, **80** [9] 862–66 (1976).
[18]O. Kubaschewski and C. B. Alcock; p. 383 in Metallurgical Thermochemistry, 5th ed. Pergamon, New York, 1979.
[19]G. L. Bullard, "Development of the High-Temperature, Solid State, Electromotive Force Technique to Study the Thermodynamics of Lewis-Acid-Base Transition Metal Alloys," LBL–7691 (1978).
[20]H. Kleykamp and A. A. Supawn, "Gibbs Energies of Formation of MoO_2 and Mo_4O_{11}," *J. Less-Common Met.*, **63**, 237–44 (1979).
[21]JANAF Thermochemical Tables, 2d ed. NSRDS–NBS 37, June 1971.
[22]R. A. Rapp, "Free Energy of Formation of Molybdenum Dioxide," *Trans. Met. Soc. AIME*, **227**, 371–74 (1963).
[23]V. N. Drobyshev, T. N. Rezukhina, and L. A. Tarasova, "Thermodynamic Properties of Alloys in the System Co-Mo," *Russ. J. Phys. Chem.*, **39** [1] 70–73 (1965).
[24]N. S. Zabeivorota, A. A. Lykasov, G. G. Mikhailov, and E. L. Shakhin, "Elasticity of Molybdenum Dioxide Dissociation," *Akad. Nauk, SSSR, Neorg. Mater.*, **13** [2] 388–90 (1977).
[25]H. Kleykamp and V. Schauer, "Phase Equilibria and Thermodynamics in the Fe-Mo and Fe-Mo-O Systems," *J. Less-Common-Met.*, **81**, 229–38 (1981).
[26]C. B. Alcock and A. Kubik, "A Thermodynamic Study of the γ Phase Solid Solutions Formed between Palladium, Platinum and Iron," *Acta Met.*, **17**, 437–42 (1969).
[27]M. H. Rand, R. J. Ackermann, F. Gronvold, F. L. Oetting, and A. Pattoret, "The Thermodynamic Properties of the Urania Phase," *Rev. Int. Hautes Temp. Refract.*, **15**, 355–65 (1978).
[28]I. Johnson, C. E. Johnson, C. E. Crouthamel, and C. A. Seils, "Oxygen Potential of Irradiated Urania Plutonia Fuel Pins," *J. Nucl. Mater.*, **48**, 21–34 (1973).
[29]H. Kleykamp, "The Radial Oxygen Distribution in the Fuel of Irradiated Fuelpins of Different Initial Stoichiometries," *J. Nucl. Mater.*, **66**, 292–300 (1977).
[30]G. J. McCarthy and M. T. Davidson, "Ceramic Nuclear Waste Forms: I, Crystal Chemistry and Phase Formation," *Am. Ceram. Soc. Bull.*, **54** [9] 782–86 (1975).